A Probabilistic Multi-scenario Assembly Point Optimization Model for Severe Nuclear Accident Evacuation

Shengyu Liu[a], Wei Wang[b]
[a] City University of Hong Kong, Hong Kong, China, sheliu6-c@my.cityu.edu.hk
[b] City University of Hong Kong, Hong Kong, China, wwang326@cityu.edu.hk

Abstract: Appropriate Assembly Point (AP) allocation in the early stage of a severe nuclear accident reduces dose risk, thereby mitigating health impacts on residents near a Nuclear Power Plant (NPP). However, existing studies focusing on limited accident scenarios restrict the robustness of AP allocation. In this study, we propose a Probabilistic Multi-scenario Assembly Point Optimization (PMAPO) framework for robust AP allocations, thereby mitigating the radiation risk of residents from their initial locations to assigned APs. First, dose distributions for multiple hypothetical scenarios are generated to establish a solid basis for risk characterization. Subsequently, a probabilistic risk metric is defined to construct a risk map based on these dose distributions for risk quantification. Finally, the NSGA-II multi-objective algorithm is applied to optimize AP allocation by minimizing cumulative dose risk and evacuation time. A case study of the Daya Bay NPP (DBNPP) demonstrates the robustness of the proposed framework, as the optimized allocation plans consistently reduce cumulative dose risk across most single scenarios.

Keywords: AP allocation optimization, probabilistic risk assessment, NSGA-II, nuclear accident

1. INTRODUCTION

Nuclear power, as a mature and non-carbon energy form, is experiencing continuous expansion worldwide, while China has planned a large number of new Nuclear Power Plants (NPPs) to be constructed in the future[1]. However, past severe nuclear accidents, for example, the Fukushima Daiichi nuclear accident, have caused significant offsite consequences on human health, economy, and environment. Such severe consequences have intensified public concern about the safety of the NPP, as the radioactive materials released from NPPs during a severe nuclear accident will influence the residents around the NPP through the inhalation of air. Emergency evacuation is an effective way to mitigate or even prevent the severe consequences of a nuclear accident, since residents move away from the dispersed radioactive plume.

The evacuation of the nuclear accident contains two phases. During the first phase, the residents around an NPP will walk from their initial locations, usually their homes, to some locations where buses will arrive, pick up these residents, and transport them to places that are far away from the NPP. These locations are called Assembly Points (APs). During the second phase of the evacuation, the residents will be picked up by buses at APs and be transported from APs to some shelters that will not be influenced by the radioactive materials in a long-term period.

The APs occupy an important role during the nuclear accident evacuation process, as they act as intermediate transfer nodes that determine the walking time of the residents and the availability of buses through their location distributions. Appropriate AP allocation during the early-stage evacuation of a severe nuclear accident can reduce the dose risk through the prevention of passing through the radioactive area. Recent studies have made a lot of effort in the allocation of the APs. Ruan et al. developed an improved NSGA-II algorithm, where a local search method has been added to reduce the probability of falling into a local optimum when solving the AP allocation problem during a nuclear accident[2]. A three-layer objective optimization model has been established to improve the evacuation efficiency by balancing the evacuation time, distance, and reliability of the bus-based evacuation during the AP and shelter allocations process under nuclear accident conditions [3]. The allocation of other types of gathering points, such as shelters, has also been studied, where the balancing of capacity, evacuation efficiency, and accessibility has been considered to provide a more balanced shelter allocation in nuclear emergencies [4]. However, these studies have focused on some static and single nuclear accident scenarios, which fail to account for the uncertainty of the radioactive plume distributions, which are caused by the uncertain distribution of the meteorology and source term. The Probabilistic Safety Assessment (PSA) method, through sampling and analyzing multiple severe nuclear accident scenarios, is an effective way to overcome the deficiency in terms of uncertainty coverage.

In this study, we proposed a Probabilistic Multi-scenario Assembly Point Optimization (PMAPO) model to establish a robust AP allocation plan through the coverage of the uncertainty of the offsite radioactive plume distributions. First, we generate multiple hypothetical severe nuclear accident release scenarios through a Monte Carlo sampling of meteorological conditions and source terms, thereby calculating their dose distributions to cover the radiological uncertainty. Then, Conditional Value at Risk (CVaR) is used as the probabilistic risk metric definition to quantify risk by constructing a risk map from the dose distributions of these release scenarios. Finally, the NSGA-II multi-objective optimization algorithm is applied to allocating the APs by minimizing the cumulative dose risk and evacuation time.

2. MATERIALS AND METHOD

In this part, the mandatory data and the PMAPO model that are used to calculate the multiple dose distributions and allocate the APs will be introduced. First, the meteorological data and source term distribution used in the dose distribution calculation and the data used in AP allocation will be introduced. Then, the generation of the multiple dispersion scenarios will be explained, where the MC sampling method adopted in this part will be introduced. The CVaR definition will be given to quantify risk and establish the risk map. Finally, the AP allocation model will be demonstrated.

2.1. Data preparation

1. Meteorological data, source term, and terrain condition
Meteorological data is used to determine the dispersion pattern of radioactive plume through the wind speed and direction, temperature, precipitation, and so on. It is provided in many online sources, where the fifth generation of ECMWF reanalysis data (ERA5) is frequently used due to its data integrity [5].

The real source term data is limited, since severe nuclear accidents are rare events. Therefore, we use hypothetical source terms, which are adapted from a level 3 PSA analysis conducted by the U.S. Nuclear Regulatory Commission [6]. The source term data includes 10 categories, where each category represents a different severity of nuclear accidents. In each Source Term Category (STC), the probability and relative probability of the STC, the total release fraction of different radionuclide inventories, and the release duration are listed in **Table 1**.

Table 1: Information on STCs

STCs	Probability	Relative probability	Release Duration (hr)	Release Fraction				
				I	*Cs*	*Xe/Kr*	*Te*	*Sr*
s_1	7×10^{-8}	1.78×10^{-3}	118	0.34	0.25	0.913	0.282	2.7×10^{-3}
s_2	6×10^{-7}	1.53×10^{-3}	157	0.23	0.09	0.951	0.187	4.7×10^{-3}
s_3	7×10^{-8}	1.78×10^{-3}	125	0.15	0.16	0.982	0.131	2.2×10^{-3}
s_4	1×10^{-7}	2.55×10^{-3}	67	0.13	0.13	0.864	0.134	2.1×10^{-3}
s_5	2×10^{-7}	5.10×10^{-3}	68	0.12	0.09	0.862	0.109	1.0×10^{-3}
s_6	9×10^{-6}	2.29×10^{-1}	124	0.04	0.03	0.988	0.043	2.0×10^{-3}
s_7	7×10^{-8}	1.78×10^{-3}	151	0.04	0.03	0.984	0.038	1.5×10^{-3}

s_8	7×10^{-8}	1.78×10^{-3}	151	0.03	0.025	0.976	0.026	7.1×10^{-4}
s_9	7×10^{-8}	1.78×10^{-3}	117	0.01	0.01	0.197	0.010	1.8×10^{-4}
s_{10}	3×10^{-5}	7.39×10^{-1}	163	0.01	0.009	0.908	0.012	3.0×10^{-4}

The terrain data is adapted from the Shuttle Radar Topography Mission (SRTM) 1 Arc-Second Global data, which offers worldwide coverage of elevation information at a resolution of 30 meters, enabling the simulation of atmospheric radionuclide dispersion under real terrain conditions [7].

2. Road, residents distribution, candidate AP.
In this work, the road data is adopted from the GRIP4 dataset, as it provides a more recent and consistent global roads dataset for use in global environmental [8].

The population data is provided in many data sources, among which the WorldPop dataset provides recent, detailed population distribution. The dataset includes the distribution of residents from 2010 to 2026, where the age and sex structures of the population are demonstrated. Therefore, we use this dataset to simulate the distribution of residents around NPPs [9].

Due to the lack of official AP location information issued by the local government, we use the bus stop near the main road, which includes the latitude and longitude, as the candidate AP locations, since these bus stops are usually designed with large spaces to provide convenience for gathering and picking up the population.

2.2. Generation and calculation of multiple dispersion scenarios

1. Scenario generation and dispersion model
The individual dispersion scenario is established by combining the meteorological sample, source term sample, and the local terrain condition. For each dispersion scenario, the computational domain is divided into a structured Cartesian grid:

$$\mathcal{G} = \{(x_p, y_q) \mid p = 1,\dots,N_x; q = 1,\dots,N_y\} \tag{1}$$

We adopt the Gaussian puff model to simulate the dispersion scenario, as it is suitable for a short and middle range of the dispersion (usually less than 300 km) [10], saving the computational resources and time while maintaining the accuracy. The CALPUFF software is used, as it is driven by input cards, which are convenient for batch writing the information of all dispersion scenarios and simulating these scenarios.

2. Dose conversion
We adopt inhalation dose coefficients to convert radionuclide concentrations of all scenarios to the temporal effective dose distributions, as inhalation has a major radioactive impact on human body health during a short period after the severe nuclear accident happens. The inhalation dose conversion factors of different radionuclides are introduced in **Table 2**.

Table 2: Dose coefficient of different radionuclides

Radionuclides z	Effective Dose Coefficient e_z (Sv/Bq)
I-131	7.4×10^{-9}
Cs-137	4.6×10^{-9}
Te-132	1.8×10^{-9}
Xe-133	1.2×10^{-9}
Kr-88	8.4×10^{-9}
Sr-90	2.4×10^{-8}

3. MC sampling
The MC sampling method is used to generate meteorological and source term samples from their distributions, respectively. A continuous distribution of the source term is first established from its

original discrete distribution, as provided in **Table 1**. Besides, the meteorological samples are generated by a randomized-start block sampling from the long-term, hourly meteorological database downloaded from the ERA5 data provider. Both the establishment process of the continuous distribution and the generating method of meteorological samples are already introduced in our previous work [11].

A two-loop MC sampling method is designed to simulate multiple spatiotemporal evolved dispersion scenarios. In the outer loop, the MC sampling will be looped J times to generate multiple scenarios. For each $j \in J$, the j-th loop contains an inner loop, where the j-th scenario is divided into N discrete time steps. For each $n \in N$, at the n-th time step, the gridded average concentration distribution $C_{x,y,z,n,j}$ ($x \in N_x$, $y \in N_y$) of each radionuclide z is calculated, which is multiplied by the corresponding dose coefficients e_z introduced in **Table 2** to obtain the time-dependent gridded dose field $E_{x,y,n,j}$. Then, we obtain gridded dose fields at all time steps $\boldsymbol{E}_{x,y,j}=\{E_{x,y,1,j}, E_{x,y,2,j}, \ldots, E_{x,y,N,j}\}$. After J times outer loop, we finally obtain the gridded dose fields at all time steps for all dispersion scenarios $\mathbf{E}_{x,y}=\{\boldsymbol{E}_{x,y,1}, \boldsymbol{E}_{x,y,2}, \ldots, \boldsymbol{E}_{x,y,J}\}$.

2.3. Risk map establishment

A CVaR definition is used to quantify the dose risk and thereby establish a risk map. The risk map establishment process is introduced below:

1. Calculate the CVaR of the dose
We set a 95% confidence interval and use this confidence interval to calculate the CVaR, which is the average of the 5% tail value.

2. Quantify the gridded time-dependent risk
Using the CVaR definition, we quantify the dose risk of each grid at each time step, by calculating the CVaR of the gridded time-dependent dose distribution from the gridded dose field in all dispersion scenarios $\mathbf{E}_{x,y}$. For each grid, the CVaR of the dose distribution at time step n is denoted as $V_{x,y,n}$.

3. Define the time-dependent gridded risk area
We compare the time-dependent gridded dose risk $V_{x,y,n}$ with a dose criterion D recommended by the ICRP [12], which is 50 mSv/week, representing that the residents around the NPP should evacuate immediately. We use a risk indicator $R_{x,y,n}$ to represent whether the grid (x, y) at the time step n is marked as a risk area:

$$R_{x,y,n} = \begin{Bmatrix} 1; V_{x,y,n} I > D \\ 0; V_{x,y,n} I < D \end{Bmatrix} \tag{2}$$

where I represents the inhalation rate, 16 m^3/day, recommended by the US Environmental Protection Agency [13]. $R_{x,y,n}$=1 represents the grid (x, y) is risky at the time step n, while $R_{x,y,n}$=0 represents the grid is not risky at this time step. By combining risk indicators of all grids, we obtain a risk field at the time step n. Finally, the time-dependent risk map can be calculated by gathering all risk fields generated by each time step.

2.4. AP allocation model

The NSGA-II algorithm is used in this work, as it is designed to solve two-objective problems, where the objectives are conflicting with each other. We introduce the assumptions, boundary conditions, and the algorithm configurations to construct the AP allocation model.

1. Assumptions
(1) All residents will fully comply with the order of the local government, which means they will follow the bus-based evacuation order, instead of using personal transportation.
(2) Residents from the same original location will walk to the same AP location.
(3) The number of available vehicles in each AP is fixed, and vehicles will arrive at various AP locations from the bus dispatch center.

(4) The traffic conditions of the road during the bus-based evacuation from APs to shelters, as these roads are assumed to be used by the evacuation buses before other transportation forms.
(5) The buses will travel back and forth until all residents in APs are evacuated.
(6) The route selection of buses is dependent on the Dijkstra algorithm.
2. Boundary conditions
(1) The walking speeds of residents are dependent on the age and structure of the residents.
(2) Residents must reach the APs within 45 minutes.
(3) Among the shelters that have not been fully occupied by residents, buses that evacuate residents will travel to the nearest one.
(4) Buses cannot reach an AP that is covered by the risk area.
(5) Buses must evacuate residents to shelters that are more than 30 km from the NPP.
3. Algorithm configuration
The NSGA-II algorithm is adopted to solve the AP allocation problem, where the configuration of the NSGA-II is presented in **Table 3**.

Table 3: Configurations of the NSGA-II algorithm

Parameters	Value
Population size	200
Number of offspring	200
Number of generations	160
Probability of crossover	0.7
Probability of mutation	0.3

Two optimization objectives have been set, which are the population-weighted risk and population-weighted walking time, to consider the trade-off between the evacuation efficiency while reducing the risk of the evacuation in the risk area. The objective function of minimizing the population-weighted walking time is shown below.

$$\min f_1 : \sum_{a=1}^{A} \sum_{e=1}^{E} \frac{B_{ea}}{V_e} \cdot D_{ea} \cdot N_e \tag{3}$$

where the f_1 and f_2 represent minimizing the population-weighted walking time and minimizing the population-weighted risk, respectively. A represents the number of allocated AP allocations; E represents the number of resident groups; V_e represents the walking speed of the resident group e; D_{ea} represents the distance between resident group e and AP location a; Ne represents the number of residents in resident group e. Each resident should be allocated to only one AP location, which is represented by a binary variable, B_{ea}:

$$\sum_{a=1}^{A} B_{ea} = 1, \forall e \in E \tag{4}$$

$$\sum_{e=1}^{E} B_{ea} > 0, \forall a \in A \tag{5}$$

The objective function of minimizing the population-weighted risk is demonstrated below:

$$\min f_2 : \sum_{n=0}^{n_e} \sum_{e \in E} N_e R_{e,n} \Delta t \tag{6}$$

where n_e represents the number of discrete time steps of the evacuation process from residents leaving their original locations to all residents being evacuated to shelters; $R_{e,n}$ represents the risk value of resident group e, which is calculated by the location of e at the n-th time step, and Δt represents the time interval of each time step.
In this work, we adopt the knee point method to select the solution from the final Pareto front. The solution selected by the knee point method represents a trade-off result, where the change of one objective value could lead to the largest change of the other objective value.

3. RESULTS AND DISCUSSIONS

In this section, the PMAPO model is applied to the case study of DBNPP, as this NPP has been operated for decades, and is situated near the population-dense cities, such as Shenzhen and Hong Kong.

3.1. Case study

As shown in **Figure 1**, the computation domain of this case study is demonstrated. The circle points with the orange color represent the residents around the DBNPP. The triangular points with green color represent the candidate AP locations, which are also marked as pickup stops in the legend of the figure. The square points with blue represent the long-term shelters in Shenzhen. The red dashed box represents the domain where residents will be evacuated, and the purple dashed box represents the domain where the spatiotemporal evolution of the dose field will be calculated.

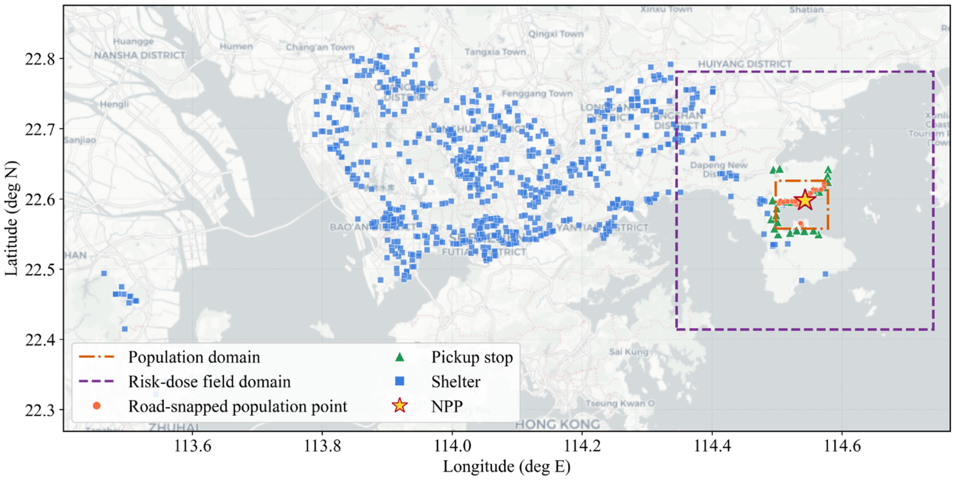

Figure 1: Computation domain of the case study

The number of buses is set to be 200. The walking speed related to the age and gender structure of the residents is adapted from a research of pedestrian mobility [14], which is shown in **Table 4**.

Table 4: Walking speed of residents in different age and gender structures

Age	20-29		30-39		40-49		50-59		60-69		70+	
Gender	M	F	M	F	M	F	M	F	M	F	M	F
Speed (m/s)	2.01	1.84	1.94	1.77	1.87	1.72	1.81	1.65	1.70	1.59	1.55	1.28

3.2. Allocation result and discussion

As shown in **Figure 2**, the final Pareto result of the NSGA-II optimization process is given, and the solution selected by the knee point method is provided, as marked in the figure.

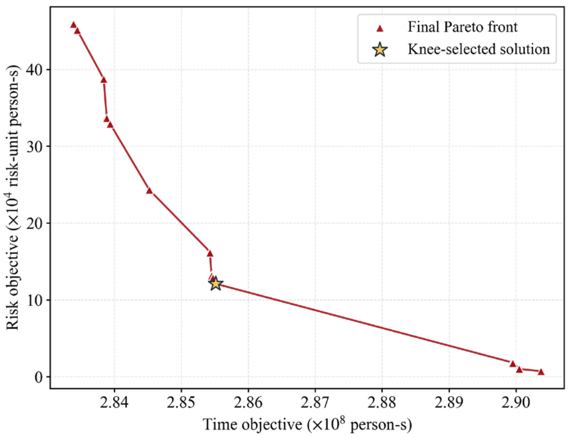

Figure 2: The final Pareto front and Pareto solution selected by the knee point method

Using this solution, the final AP allocation results and the shelter adoption results are demonstrated in **Figure 3** and **Figure 4**. The triangular marks shown in **Figure 3** represent the APs that are adopted to receive the residents, which are marked by red circles. The size of the AP marks represents the number of residents they collect, where a larger size represents more residents, and a smaller size represents fewer residents. The star represents the location of DBNPP, where the radioactive plume will be dispersed. The 45-min risk area, defined by the CvaR, is distributed in the Northeast-Southwest direction, which is due to the prevailing wind direction of the Daya Bay area. Therefore, APs that fall into this area have been filtered so that they cannot be accessed by buses. At the AP locations that are very near the risk area, the number of residents is less than that of more distant AP locations, while the resident numbers will decrease as the distance between APs and the NPP increases. This can be attributed to the balance of the evacuation time and risk. The cumulative risk can be higher at locations near the risk area. Therefore, increasing the distance between APs and the risk area or the NPP can decrease the population-weighted cumulative risk. As the distance increases, the population-weighted walking time will increase, which is against the optimization objective. As shown in **Figure 4**, the square marks represent the shelters adopted in this optimization process, while the size of these shelters represents the number of residents they received. The route between APs and shelters adopted by buses are shown in this figure.

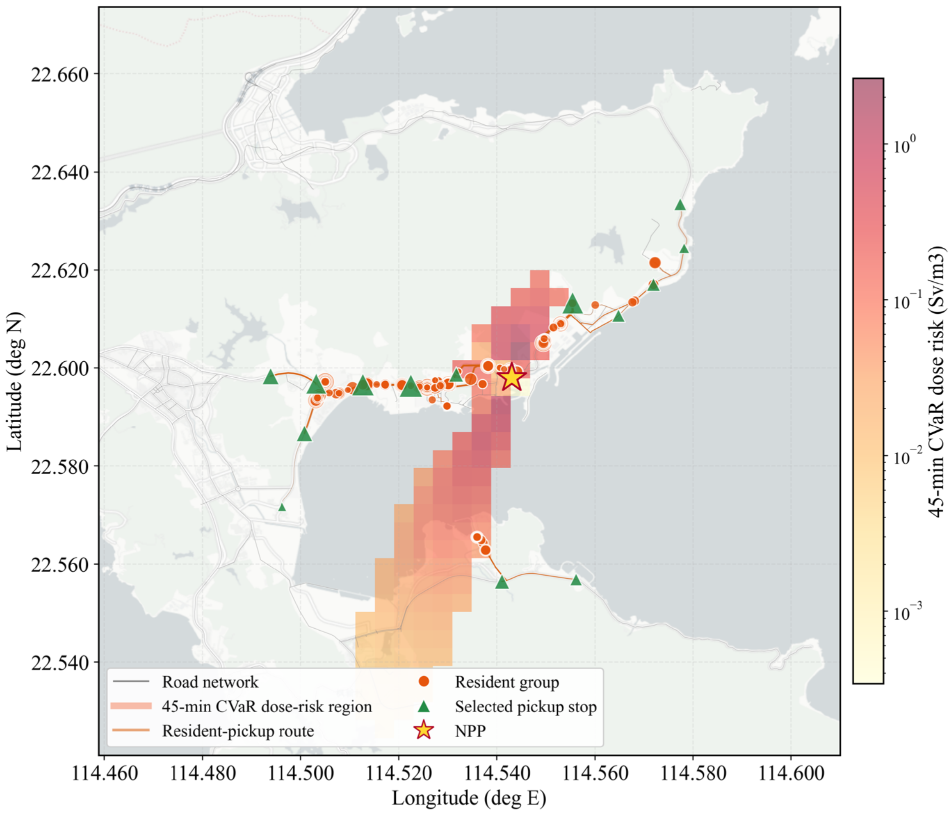

Figure 3: AP Allocation result

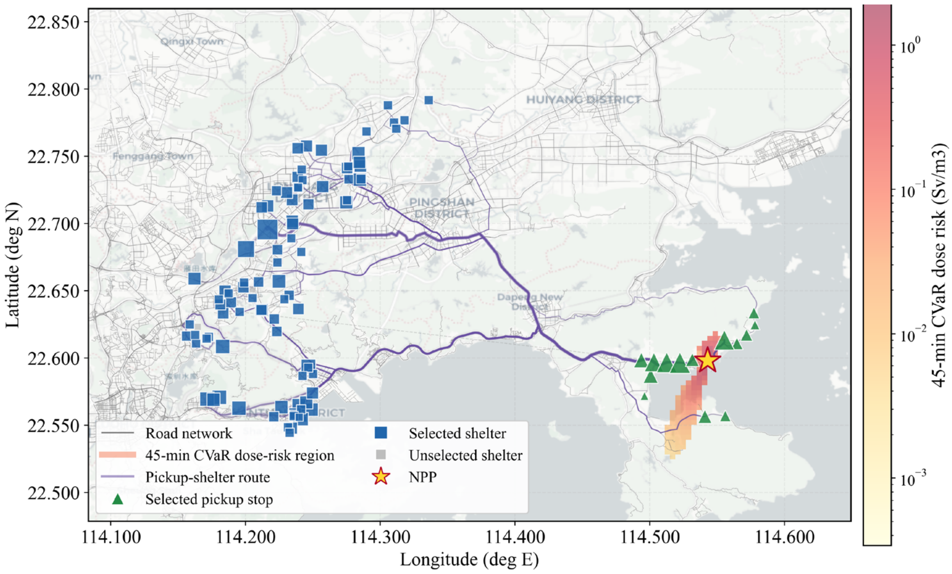

Figure 4: The AP and shelter adoption result

4. CONCLUSION

In this work, a PMAPO model is established to provide a robust AP allocation plan through the coverage of the uncertainty of the offsite radioactive plume distributions. The conclusions of this work are summarized below:

(1) The PMAPO model provides robust AP allocation results by allocating residents to the APs that will not be affected by the risk area defined by the PMAPO model.

(2) The risk map shows that the risk around DBNPP is mainly distributed along the Northeast-Southwest direction, filtering the AP locations in this direction, due to the prevailing wind directions in this area.

Acknowledgements

The authors gratefully acknowledge the financial supports of this work by the Research Grants Council of Hong Kong under the grant No. 11215323, the Science, Technology and Innovation Bureau of Shenzhen Municipality under the grant No. JCYJ20250604184535045, and City University of Hong Kong under the grant No. 9610599.

References

[1] INTERNATIONAL ATOMIC ENERGY AGENCY, *Nuclear power reactors in the world*. in Reference Data Series. INTERNATIONAL ATOMIC ENERGY AGENCY, 2025.

[2] F. Ruan, C. Chen, C. He, Y. Cheng, and Y. Sun, “Optimization method of public decontamination location and allocation problem in off-site nuclear emergency based improved NSGA-II,” *Journal of Hazardous Materials*, vol. 489, p. 137572, Jun. 2025.

[3] Y. Sun, X. Chai, and C. Chen, “Bus based emergency evacuation organization strategy of nuclear power plant planning restricted area,” *Progress in Nuclear Energy*, vol. 169, p. 105081, Apr. 2024.

[4] Y. Sun, T. Wu, H. Ren, B. Ding, and X. Chai, “Emergency evacuation model of nuclear power plant pedestrians considering emotional infection,” *Ann. Nucl. Energy*, vol. 224, p. 111683, Dec. 2025.

[5] C. Soci *et al.*, “The ERA5 global reanalysis from 1940 to 2022,” *Quart J Royal Meteoro Soc*, vol. 150, no. 764, pp. 4014–4048, Oct. 2024.

[6] “U.S. NRC level 3 probabilistic risk assessment (PRA) project, volume 3D: Reactor, at-power, level 3 PRA for internal events and floods.

[7] “Shuttle radar topography mission 1 arc-second global.” 2021.

[8] J. R. Meijer, M. A. J. Huijbregts, K. C. G. J. Schotten, and A. M. Schipper, “Global patterns of current and future road infrastructure,” *Environ. Res. Lett.*, vol. 13, no. 6, p. 064006, Jun. 2018.
[9] M. Bondarenko *et al.*, “Constrained estimates of 2015-2030 total number of people per grid square at a resolution of 3 arc (approximately 100m at the equator) R2025A version v1.” 2025.
[10] A. Hernández-Garces, J. A. G. Reynoso, and Y. Morera-Gómez, “Impact of radioactive emissions from the laguna verde nuclear power plant using CALPUFF,” *Ann. Nucl. Energy*, vol. 205, p. 110603, Sep. 2024.
[11] S. Liu, H. Ding, A. Hu, G. Wu, S. Fang, and W. Wang, “Off-site risk area delineation under severe nuclear accident conditions: A deterministic-probabilistic coupled consequence analysis,” *Journal of Hazardous Materials*, vol. 511, p. 142181, Jun. 2026.
[12] J. Vennart, “The 1990 recommendations of the international commission on radiological protection,” *J. Radiol. Prot.*, vol. 11, no. 3, pp. 199–203, Sep. 1991.
[13] “Exposure factors handbook - chapter 6: Inhalation rates”.
[14] E. M. Barnes, “Realistic evacuation simulation through micro and macro scale agent-based modelling including demographics, agent patience and evacuation route capacities”.